RESEARCH ARTICLE

Occludin, caveolin-1, and Alix form a multi-protein complex and regulate HIV-1 infection of brain pericytes

Silvia Torices | Samantha A. Roberts | Minseon Park | Arun Malhotra |
Michal Toborek

Department of Biochemistry and Molecular Biology, University of Miami Miller School of Medicine, Miami, FL, USA

Correspondence
Michal Toborek and Silvia Torices, Department of Biochemistry and Molecular Biology, University of Miami Miller School of Medicine, 528 Gautier Bldg, 1011 NW 15th Street, Miami, FL, USA.
Email: mtoborek@med.miami.edu (M. T.) and sxt736@med.miami.edu (S. T.)

Abstract

HIV-1 enters the brain by altering properties of the blood-brain barrier (BBB). Recent evidence indicates that among cells of the BBB, pericytes are prone to HIV-1 infection. Occludin (ocln) and caveolin-1 (cav-1) are critical determinants of BBB integrity that can regulate barrier properties of the BBB in response to HIV-1 infection. Additionally, Alix is an early acting endosomal factor involved in HIV-1 budding from the cells. The aim of the present study was to evaluate the role of cav-1, ocln, and Alix in HIV-1 infection of brain pericytes. Our results indicated that cav-1, ocln, and Alix form a multi-protein complex in which they cross-regulate each other's expression. Importantly, the stability of this complex was affected by HIV-1 infection. Modifications of the complex resulted in diminished HIV-1 infection and alterations of the cytokine profile produced by brain pericytes. These results identify a novel mechanism involved in HIV-1 infection contributing to a better understanding of the HIV-1 pathology and the associated neuroinflammatory responses.

KEYWORDS

Alix, blood-brain barrier, caveolin-1, HIV-1, pericytes

1 | INTRODUCTION

Pericytes are multifunctional mural cells that surround microvessels and are often in direct cellular contact with endothelial cells.[1,2] They cover 30% of the abluminal surface of endothelial cells in peripheral capillaries[3] and over 90% of brain capillaries.[4] By coordinating functions with endothelial cells, neurons, and astrocytes, pericytes have recently attracted significant attention for regulating the development, functional integrity, and the maintenance of blood-brain barrier (BBB).[5-8] In addition, pericytes play a critical role in capillary blood flow,[9] blood vessel development,[9] angiogenesis, and neuroinflammation.[10,11] It was proposed that identifying functions and the behavior of brain pericyte can be a key factor in better understanding the pathology underlying several neurological diseases, including neuroinfections.[12-15]

Abbreviations: BBB, blood-brain barrier; CAV-1, caveolin-1; ESCRT, endosomal sorting complexes required for transport; HEK, human embryonic kidney; OCLN, occludin; PRD, proline rich domain; RIPA, radioimmunoprecipitation assay; TJ, tight junction.

HIV-1 is known to penetrate into the CNS as the result of the systemic infection in a process that includes alterations of the structural integrity of the BBB.[16] One of the most important features of the BBB is the existence of high-resistance interendothelial tight junctions (TJs). They are formed by integral membrane proteins, such as claudins, occludin (ocln), and cytoplasmic proteins (eg, zonula occludens proteins) that act as structural components by limiting paracellular permeability via closing the gaps between adjacent endothelial cells.[17,18] While it is believed that HIV-1 disrupts the BBB permeability by functional and structural hindrance of TJs, recent evidence indicates that HIV-1 can also infect brain pericytes.[19-23] Infected pericytes can release the virus into the microenvironment, potentially providing a previously unrecognized mechanism of HIV-1 entry into the CNS directly related to pathobiology of the BBB.[20-22]

Occludin (ocln) is a transmembrane TJ protein[24]; however, recent evidence has shown an important role of this protein in regulating cellular metabolism through influencing AMPK protein kinase activity, ATP production, and glucose uptake.[25] Importantly, ocln can control the responses of human pericytes to HIV-1 and influence the level of infection.[20] Another membrane protein that is involved both in maintaining BBB integrity and HIV-1 infection is caveolin-1 (cav-1).[26-28] Cav-1 is the major structural protein of the caveolae and lipid rafts, where it plays a key role in regulation of raft-dependent endocytosis.[29] As such, it is involved in multiple cellular processes that include angiogenesis, signal transduction, inflammation, cellular senescence, lipid regulation, cancer, and apoptosis.[30-35] Studies have also related cav-1-mediated endocytosis to epithelial TJ dynamics.[36]

One of the essential phases of the viral life cycle is the budding and release of viral particles from infected cell. Retroviruses, such as HIV-1, evolved the ability to modify the machinery of target cells in order to promote viral egress from the cell. While it is known that this process involves endosomal sorting complexes required for transport (ESCRT) proteins and pathways, the associated machinery of HIV-1 release is still poorly understood and has never been studied in HIV-1-infected brain pericytes. Alix is an early acting ESCRT factor that plays a direct role in exosome biogenesis[37] and is involved in HIV-1 budding from the cells.[38,39] As a multidomain adaptor protein, Alix binds to the viral Gag protein which recruits the ESCRT factor to facilitate membrane fission and virion release.[40]

The goal of the present study was to evaluate the role of proteins involved in membrane plasticity during HIV-1 infection of human brain pericytes. Our results demonstrate for the first time that cav-1, ocln, and Alix form a complex that is affected as a result of pericytes infection with HIV-1. Importantly, modifications of this complex can regulate the rate of HIV-1 infection and egress from infected cells.

2 | MATERIALS AND METHODS

2.1 | Cell culture

Primary human brain vascular pericytes (ScienCell, Carlsbad, CA, USA, Cat# 1200) belonging to five different lots were maintained in pericyte-specific growth medium (ScienCell, Cat# 1201) supplemented with fetal bovine serum (FBS; 2%), growth factors, 100 units/mL of penicillin, and 100 µg/mL of streptomycin. Cells were used from passages 2 to 7. Human embryonic kidney (HEK)-293T cells (ATCC, Manassas, VA, USA, Cat# CRL-11268) were cultured in DMEM (Thermo Fisher Scientific, Carlsbad, CA, USA, Cat#11995-065) supplemented with 10% of FBS (ScienCell, Cat# 0500), penicillin 100 units/mL, and 100 µg/mL of streptomycin (Thermo Fisher Scientific, Cat# 15140-122). Cultures were maintained in 5% of CO_2 at 37°C.

2.2 | HIV-1 production, infection, and quantitation

HIV-1 pNL4-3 was obtained from the NIH AIDS Reagent Program (Division of AIDS, NIAID, National Institutes of Health). HIV-1 pNL4-3 encoding interdomain green fluorescent protein (iGFP) was kindly provided by Dr Mario Stevenson (University of Miami, Florida, FL, USA). Viral stocks were produced in HEK-293T cells by transfection with 50 µg of proviral DNA plasmid per 10^7 cells using Lipofectamine 2000 (Thermo Fisher Scientific, Cat# 11668-027). After 24 hours, medium was changed to Opti-MEM (Thermo Fisher Scientific, Cat# 11058-021). Two days later, supernatants were collected, filtered using 0.45 µm-pore size filter (Millipore Sigma, Massachusetts, MA, USA, cat# 430314), concentrated using weight exclusion columns (Millipore Sigma, Cat# UFC905024), aliquoted, and stored in −80°C. p24 antigen, the major structural component of HIV-1, was analyzed in cell culture media for quantification of HIV-1 production using HIV-1 p24 Antigen ELISA 2.0 according to the manufacturer's instructions (ZeptoMetrix, Buffalo, NY, USA, Cat# 0801008). Pericytes were infected by incubation with 60 ng/mL of HIV-1 p24.

2.3 | Gene overexpression and silencing

Cav-1, ocln, and Alix silencing was performance using the following small interfering RNA (siRNA): anti-occludin 27-mer siRNA (h): Cat# SR321170, anti-caveolin-1 27-mer siRNA (h): Cat# SR319567 (OriGene, Rockville, MD, USA), and anti-Alix siRNA (h): Cat# sc-60149 (Santa Cruz Biotechnology, Dallas, TX, USA). Trilencer-27 universal

scrambled (SCR) silencer negative control siRNA Cat# SR30004 (OriGene) was used as nonspecific control siRNA. Pericytes were transfected by Amaxa Nucleofector Technology with 1 µg siRNA or control siRNA per 10^6 cells using the Basic Nucleofector Kit originally designed for primary mammalian endothelial cells (Lonza, Switzerland, EU, Cat# VPI-1001). Next day, cells were washed and allowed to recover in normal pericyte medium. For ocln overexpression experiments, ocln cDNA cloned into the pCMV6 plasmid was obtained from OriGene (Cat# RC206468). As a negative control, the pCMV6 plasmid (OriGene Cat# PS100001) was used. Cells were transfected with 2 µg of ocln overexpressing vector per 10^6 cells or negative control vector by using Amaxa Nucleofector Technology.

2.4 | Immunoblotting

Pericytes were washed with phosphate-buffered saline (PBS) and lysed using Radioimmunoprecipitation Assay (RIPA) buffer (Santa Cruz Biotechnology, Germany, EU, Cat# sc-24948a) with protease inhibitors. Protein concentration was measured using BCA Protein Assay Kit (Thermo Fisher Scientific, Cat# 23223). All samples were separated on a 4%-20% Mini-PROTEAN TGX Stain-Free Protein Gels (Bio-Rad Laboratories, Hercules, CA, USA Cat# 4568094) and electrotransferred onto PVDF membrane using the Trans-Blot Turbo Transfer System (Bio-Rad Laboratories, Cat# 170-4159). The blots were blocked with 5% of bovine serum album (BSA, Sigma-Aldrich, San Luis, MO, USA, Cat# A7906-500G) and incubated overnight at 4°C with the following primary antibodies (1:1000): mouse anti-Alix (Bio-Rad Laboratories, Cat# VMA00273); rabbit anti-Alix (Invitrogen, Carlsbad, CA, USA, Cat # PA5-52873); rabbit anti-occludin (Thermo Fisher Scientific, Cat# 71-1500); mouse anti-occludin (Thermo Fisher Scientific, Cat# 33-1500); rabbit anti-caveolin-1 (Thermo Fisher Scientific, Cat# PA1-064); and mouse anti-caveolin-1 (BD Biosciences, San Jose, CA, USA, Cat# 610058) in 5% of BSA-TBS. The next day, samples were washed three times with TBS-0.05% of Tween 20 for 5 minutes and incubated for 1 hour with secondary antibody (1:20 000, LI-COR, Lincoln, NE, USA, Cat# 926-32210, Cat# 926-68070, Cat# 926-32211, cat# 926-68071) in 5% of BSA-TBS. After three times washes with TBS-0.05% of Tween 20, immunoblots were visualized by Licor CLX imaging system. Image Studio 4.0 software (LI-COR) was used for signal quantification. Target protein levels were normalized to anti-GAPDH (1:20 000, Novus Biologicals Cat# NB600-502FR or Cat# NB600-5021R) or rabbit polyclonal anti-α-tubulin antibody (1:1000, Thermo Fisher Scientific, Cat# 11224-1-AP).

2.5 | Immunoprecipitation

Pericytes were lysed in NP-40 buffer containing fresh added protease and phosphatase inhibitor cocktail solution (Roche, Basel, Switzerland, EU, Cat# 11697498001). A total of 600 µg of protein lysate was incubated with 1 µg of rabbit anti-caveolin-1 antibody (Thermo Fisher Scientific, Cat# PA1-064) with gentle rotation. After 24 hours rotation, the samples were incubated for 1 hour with 25 µL protein A/G PLUS-Agarose (Santa Cruz Biotechnology, Cat# sc-2003). To collect the immune complex, samples were centrifuged at 5000 rpm for 3 minutes, and both the pellets and the supernatants were collected. The immunoprecipitates were washed three times in NP-40 lysis buffer and analyzed by immunoblotting. GAPDH was analyzed as control.

2.6 | Immunofluorescence

Pericytes were grown on a glass coverslip coated with 10 mg/mL of poly-L-lysine (Millipore Sigma, Cat# P8920). To visualize cellular membranes, cells were incubated for 20 minutes at 37°C with the CellBrite DiB Blue Cytoplasmic Membrane Dye (Biotium, Fremont, CA, USA, Cat# 30024), followed by washing three times with pericytes growth medium. Cells were fixed with 4% of paraformaldehyde for 15 minutes and permeabilized with PBS containing 0.2% of Triton X-100 for 15 minutes. To prevent nonspecific binding, cells were washed with PBS and blocked for 1 hour with 3% of BSA in TBS. Coverslips were then incubated with rabbit anti-caveolin-1 antibody (Thermo Fisher Scientific, Cat# AP1-064), or mouse anti-Alix (Bio-Rad Laboratories, Cat# VMA00273), overnight at 4°C in a humidified atmosphere. All antibodies were diluted at 1:100 in 3% of BSA in TBS. After the excess of the primary antibody was removed, the slides were washed three times with PBS and incubated for 1 hour with Alexa Fluor 488- (Thermo Fisher Scientific, Cat# A12379) or 647- (Thermo Fisher Scientific, Cat# A31571) secondary antibodies (1:400 in 3% BSA in TBS, Thermo Fisher Scientific). Next day, coverslips were incubated with mouse anti-occludin 594 conjugate antibody (1:100, Thermo Fisher Scientific, Cat# 331594) overnight at 4°C in a humidified atmosphere. The coverslips were washed three times with PBS and mounted with ProLong Diamond Antifade Mountant (Thermo Fisher Scientific, Cat# P36961) or Vectashield Antifade Mounting Medium with DAPI to visualize the nuclei (Vector laboratories, Burlingame, CA, USA, Cat# H-1500). The images were captured with Olympus FLUOVIEW 1200 Laser Scanning Confocal Microscope (Olympus, Center Valley, PA, USA).

2.7 | Multiplex cytokine assay ELISA

The quantitative determination of inflammatory cytokines in culture medium was performed using a Bio-Plex Pro Human Cytokine 27-plex Assay with a Bio-Plex MAGPIX multiplex reader (Bio-Rad Laboratories, Cat# M500KCAF0Y). The assay was conducted in a 96-well plate according to the manufacturer's instructions, and the levels of cytokines were calculated in pg/mL.

2.8 | Statistical analysis

Statistical analyses were performed with GraphPad Prism 6 (GraphPad Software, La Jolla, CA, USA). Statistical significance between the control and experimental group in vitro analyses was performed by using the two-way ANOVA following by Turkey's multiple comparisons test or Student's t-test. The significance level was set at $P < .05$.

3 | RESULTS

3.1 | HIV-1 infection affects cav-1, ocln, and Alix expression in brain pericytes

We first evaluated the impact of HIV-1 infection on expression of cav-1, ocln, and Alix in brain pericytes. The cells were mock-infected or infected with HIV-1 for 48 or 72 hours, and the expression of targeted proteins was evaluated by immunoblotting. These experimental time points were based on earlier results from the laboratory that demonstrated that HIV infection in brain pericytes results in a dual-stage response pattern influenced by occludin expression levels and picks at 48 hours.[11,20] After 48 hours infection, a significant decrease in ocln levels and an increase in the expression levels of Alix were observed. No changes, however, were found in cav-1 expression (Figure 1A). Conversely, the levels of cav-1, ocln, and Alix were all elevated when pericytes were infected by HIV-1 for 72 hours (Figure 1B), indicating that the levels of these proteins fluctuate in the course of infection. The kinetics of ocln, cav-1, and Alix changes were confirmed by immunostaining 48 and 72 hours post HIV-1 infection (Figure 1C).

3.2 | Cav-1, ocln, and Alix form a multi-protein complex in mock-infected and HIV-1-infected brain pericytes

Taking into consideration that a) the expression of cav-1, ocln, and Alix is modified by HIV-1, b) all three proteins are involved in HIV-1 infection, and c) all three proteins also play a role in membrane plasticity, we investigated if they could interact among themselves and form a complex. Indeed, Alix is an all-helical protein with multiple charged patches. It is likely that these charged patches may allow Alix binding to tyrosine motifs in helical bundles in ocln and cav-1 (Figure 2A).

The lysates of mock-infected pericytes were incubated with cav-1-antibody, and the precipitates were probed for the presence of ocln and Alix. The results of these co-immunoprecipitation studies strongly suggested that cav-1, ocln, and Alix can form a multi-protein complex (Figure 2B). Indeed, both ocln and Alix were found in cav-1 precipitates. Moreover, no traces of ocln or Alix were determined in the supernatants post co-immunoprecipitation, indicating a high-efficiency binding with cav-1 (Figure 2B). In the next series of experiments, we evaluated if this complex can be affected in pericytes infected with HIV-1. Brain pericytes were infected with HIV-1 for 48 hours, followed by immunoprecipitation of cell lysates with anti-cav-1 antibody and probing the precipitates for ocln and Alix. As indicated in Figure 2C, the formation of the cav-1-ocln-Alix complex was not affected by HIV-1 infection, mirroring the results from mock-infected pericytes. To support these results, we next performed immunostaining assay on both mock-infected and infected pericytes (Figure 2D,E). As illustrated, several focal colocalization spots between cav-1, ocln, and Alix were identified, confirming spatial interactions between these proteins (arrows in Figure 2D,E). The complex is localized primarily to the membrane and submembrane compartments in mock-infected cells. Following HIV-1 infection, the colocalization spots between cav-1, ocln, and Alix appear also in the cytoplasm, potentially reflecting the intracellular movements of these proteins during the infection (Figure 2E).

3.3 | Cav-1, ocln, and Alix regulate each other expression

After noting that cav-1, ocln, and Alix form a complex in human brain pericytes, we investigated the molecular interactions between these proteins and their impact on each other's expression. We also evaluated if interactions between these proteins could be affected in HIV-1-infected pericytes. Pericytes were transfected either with cav-1 siRNA, an ocln expression vector, or Alix siRNA. Cells were then either mock-infected or infected with HIV-1 for 48 hours, and the expression of individual proteins was evaluated by immunoblotting (Figures 3-5).

Cav-1 silencing was effective in both mock and HIV-1-infected cultures, decreasing cav-1 expression by 81% and 80%, respectively (Figure 3A,B). In mock-infected cells, cav-1 knockdown significantly increased ocln levels by 99%; an effect that was significantly attenuated upon infection with HIV-1 (an increase by only 31%) (Figure 3C). Conversely,
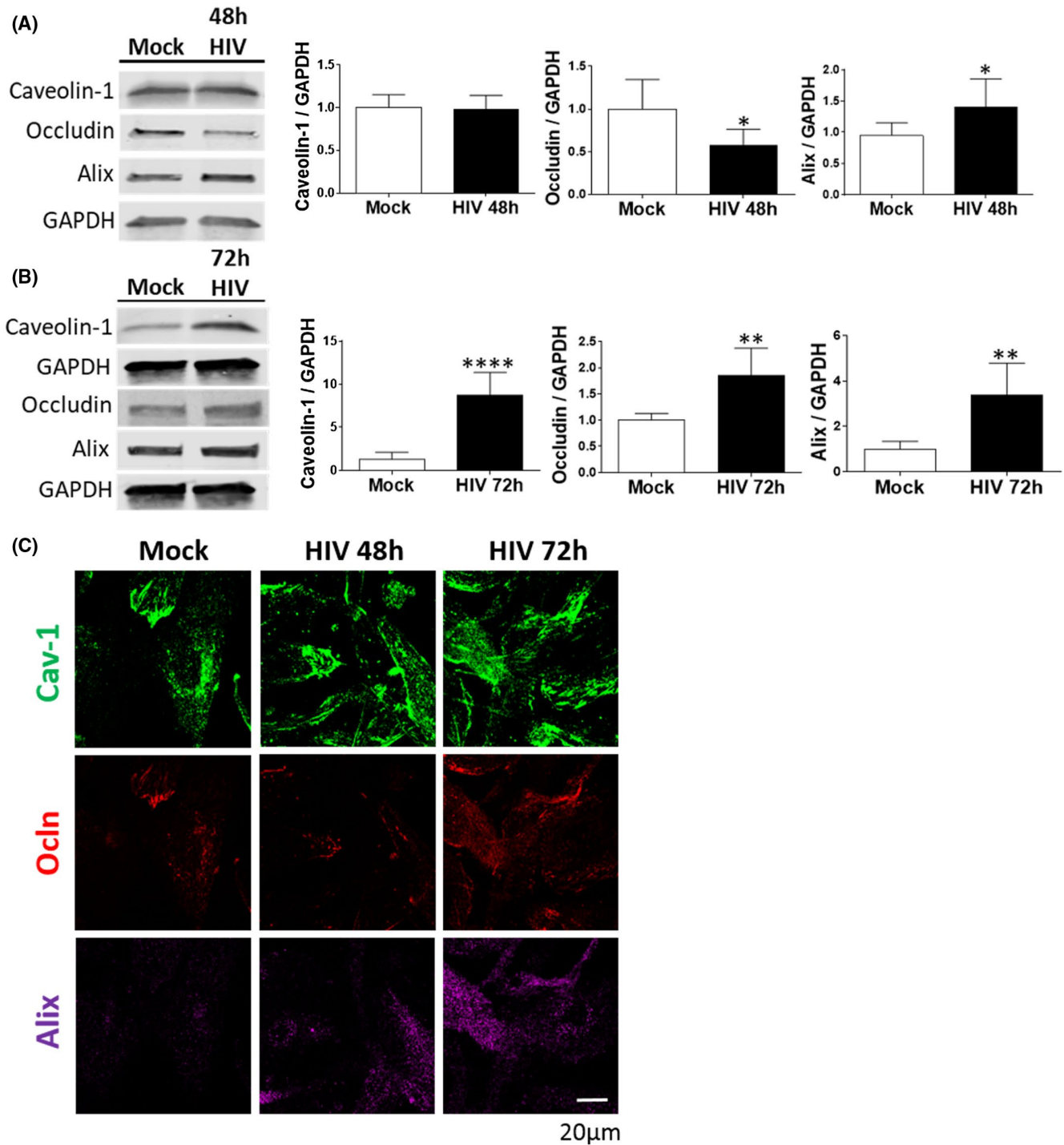
FIGURE 1 HIV-1 infection alters cav-1, ocln, and Alix expression in brain pericytes. Pericytes were either mock-infected or infected with 60 ng/mL HIV-1 p24 for 48 h (A) or 72 h (B). The expression of cav-1, ocln, and Alix was evaluated by immunoblotting. GAPDH was used as a loading control. C, Representative immunostaining images of cav-1 (green), ocln (red), and Alix (purple) in mock-infected or HIV-1-infected for 48 or 72 h. Alix expression intensity was increased by the same factors in all groups to allow for better visualization. Graphs show the mean ± SD from three independent experiments. ****$P < .0001$, **$P = .003$, *$P < .0449$, n = 4-9 per group; scale bars, 20 μm

cav-1 silencing was ineffective in changing Alix expression in both mock and HIV-1-infected pericytes (Figure 3D).

Effectiveness of ocln overexpression is illustrated in Figure 4A,B. Upon transfection with ocln expression vector,

ocln levels increased by 1200% in mock-infected cells and by 900% in HIV-infected cultures. Ocln overexpression significantly decreased protein expression of cav-1 by 32% (Figure 4C) in mock-infected pericytes. Importantly,
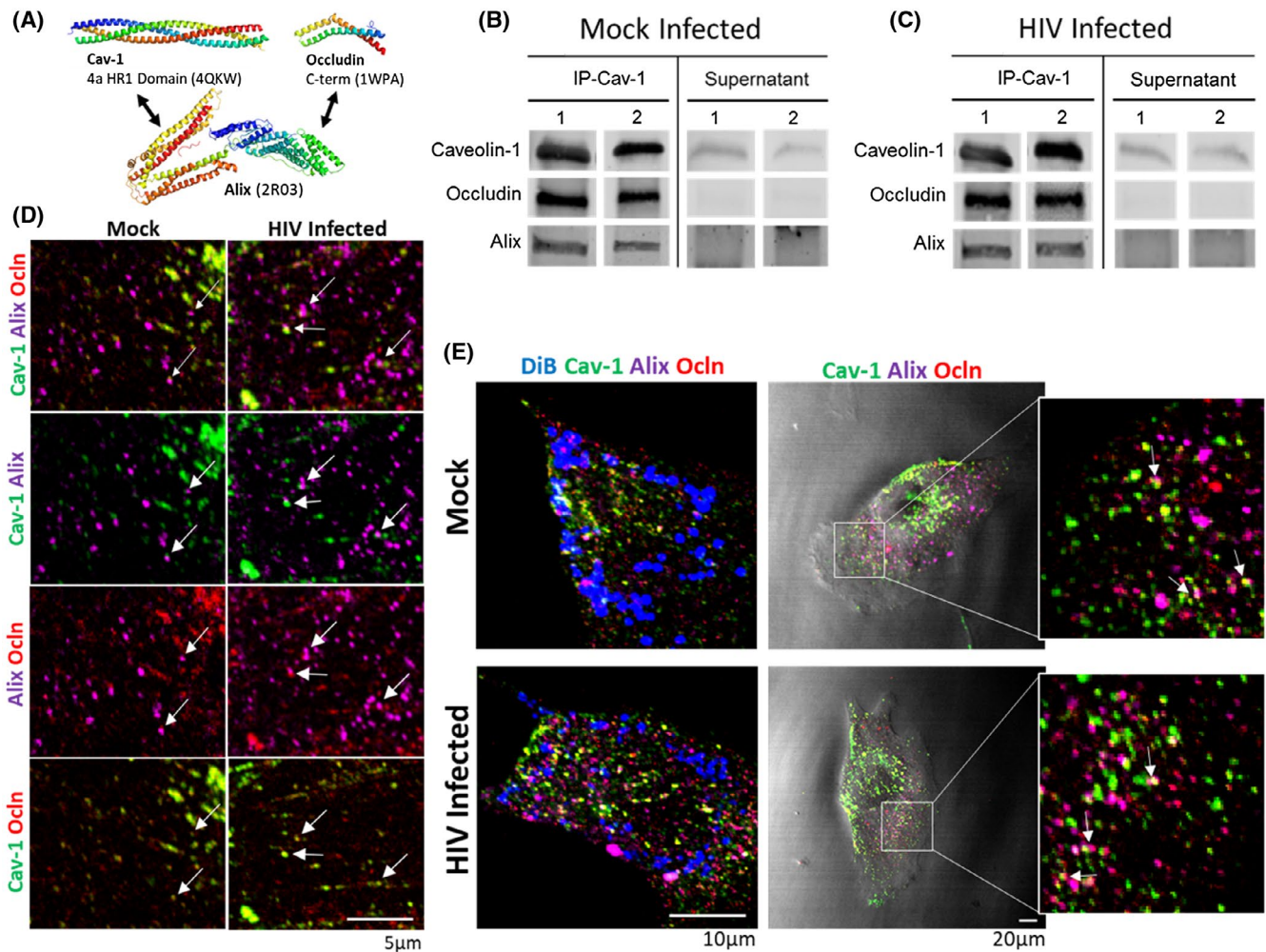
FIGURE 2 Cav-1, ocln, and Alix form a stable complex in mock-infected and HIV-1-infected pericytes. A, Diagram illustrating Alix and its binding partners identified in this study in a structural ribbon representation. The ESCRT-associated protein Alix binds tyrosine motifs via its C-terminal Proline Rich Domain (PRD). Caveolae are made up of oligomers of cav-1 and cavin proteins, and the figure shows a trimeric coiled coil for Cavin4a HR1 domain. For ocln, the region shown is the cytoplasmic C-terminal region that is known to bind scaffolding proteins. Figure was prepared using PyMol with the listed PDB accession numbers. B-E, Pericytes were either mock-infected (B) or infected with HIV-1 (C) for 48 h as in Figure 1. A total of 600 μg of cell lysate protein was incubated with cav-1 antibody for 24 h, followed by incubation with protein A/G PLUS-Agarose beads. Both immunoprecipitates and supernatants were analyzed by immunoblotting for the presence of cav-1, ocln, and Alix. D, Immunostaining of cav-1 (green), ocln (red), and Alix (purple) in mock-infected or HIV-1-infected for 48 h. E, Cellular localization of the cav-1, ocln, and Alix complex in mock-infected or HIV-1-infected for 48 h. Cell membranes are visualized by blue fluorescent dye DiB (left panel). Middle panel, the cav-1, ocln, and Alix complexes merged with a bright field image of a single pericyte. The images were analyzed as in Figure 1; n = 4 per group; scale bar 5, 10, or 20 μm

this impact on downregulation of cav-1 was not observed in ocln-overexpressing pericytes upon HIV-1 infection (Figure 4B). Ocln overexpression did not affect Alix expression (Figure 4C).

Silencing of Alix decreased its protein level by 51% in mock-infected and by 62% in HIV-1-infected pericytes (Figure 5A,B). Alix downregulation significantly decreased ocln protein expression in mock-infected cells by 26%; however, this effect was not observed when pericytes were infected with HIV-1 (Figure 5C). Silencing of Alix did not affect cav-1 protein levels in both mock-infected and HIV-1-infected cells (Figure 5D).

3.4 | Modifications of the cav-1, ocln, and Alix complex regulates HIV-1 infection and egress

In order to address the importance of the cav-1-ocln-Alix complex in HIV-1 pathology, we evaluated whether its modifications could modulate HIV-1 infection. Specifically, p24 was analyzed as the marker of active HIV replication in the supernatants of cell cultures with silenced cav-1, overexpressed ocln, and/or silenced Alix, and infected with HIV-1. The results indicate that all employed manipulations of the cav-1-ocln-Alix complex resulted in
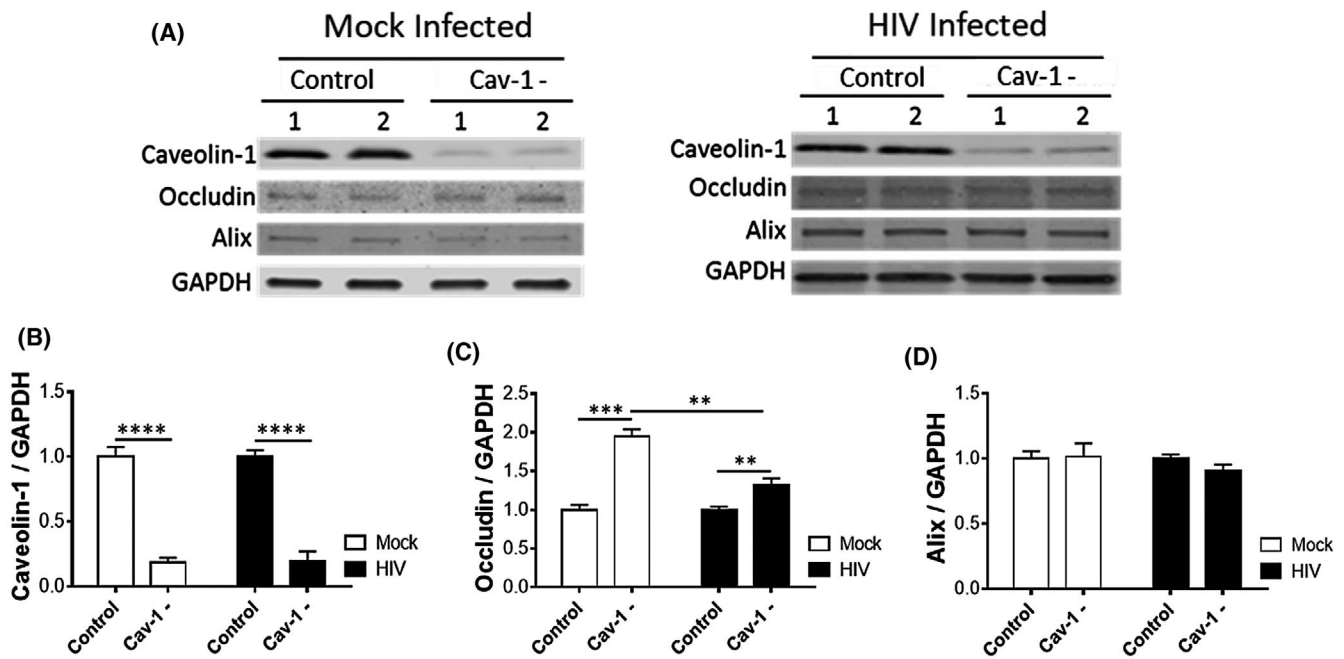
FIGURE 3 HIV-1 infection attenuates cav-1-mediated regulation of ocln expression. Pericytes were transfected with 1 µg cav-1 siRNA per 10^6 cells and either mock-infected or HIV-1-infected with 60 ng/mL HIV-1 p24 for 48 h. The expression of cav-1, ocln, and Alix was evaluated by immunoblotting (A), quantified, and compared among groups. GAPDH was used as a loading control. Cav-1 silencing (B) resulted in upregulation of occludin levels in mock-infected pericytes and this effect was attenuated in HIV-1-infected pericytes (C). Cav-1 silencing did not affect Alix levels (D). Graphs indicate the mean ± SD from three independent experiments. ****$P < .0001$, ***$P = .0002$, **$P = .003$, n = 4-9 per group

downregulation of p24 levels in cell culture media, indicating diminished HIV-1 replication (Figure 6A). When all three factors were employed together (the last bar on Figure 6A), there was no potentiation of the effect as compared to treatments with these agents alone. However, individual siRNA and occludin-overexpression construct were employed at half concentrations in this combined treatment (0.5 µg cav-1 and Alix siRNA each, plus 1 µg pCDNA-occludin per 10^6 cells) as compared to single treatments in order to avoid cell toxicity (1 µg siRNAs and 1 µg pCDNA-occludin per 10^6 cells).

We then exposed new cultures of mock-infected pericytes to the conditioned media obtained from HIV-1-infected pericyte cultures from Figure 6A. As shown in Figure 6B, exposure to conditioned media increased p24 production, indicating that HIV-1 particles generated in Figure 6A were released to cell culture media and retained their infectivity. The most pronounced infection was observed when brain pericytes were exposed to the conditioned medium collected from HIV-1-infected wild-type pericytes. Conditioned media collected from infected pericyte cultures subjected to silencing of cav-1, overexpression of ocln, and/or silencing Alix were less infectious (Figure 6B), largely mirroring the results from Figure 6A.

We also infected wild-type pericytes and pericytes with silenced cav-1, overexpressed ocln, and/or silenced Alix with HIV-1 pNL4-3 engineered to encode interdomain GFP

as a transcriptional reporter (Figure 6C). Then, HIV-1 transcription efficiency was quantified by GFP fluorescence (Figure 6D). The results indicate a significant reduction in HIV-1 transcriptional efficiency as the outcome of the employed cav-1, ocln, or Alix modifications. Similar to the results in Figure 6A,B, Acombined exposure to all three factors did not potentiate the effect on HIV-1 infection as compared to single treatments. However, like Figure 6A, siRNAs and the ocln overexpression construct were used at half concentrations in the combined experiments in order to avoid cell toxicity.

3.5 | HIV-1 infection and/or modulation of the cav-1-ocln-Alix complex affect cytokine production by brain pericytes

HIV-1 infection and/or disruption of the BBB integrity promote neuroinflammatory responses; processes that are consistent with the observations that patients living with HIV-1 suffer from inflammatory conditions.[41] Therefore, we evaluated the impact of the modification of the cav-1, ocln, Alix complex on pro-inflammatory responses in mock-infected and HIV-1-infected pericytes. A total of 27 inflammatory cytokines were analyzed in cell culture media using a customized Cytokines Multi-Analyte ELISArray Kit. The levels of IL-13, GM-CSF, IL-1β, IL-4, IL-8, and MIP-1α were
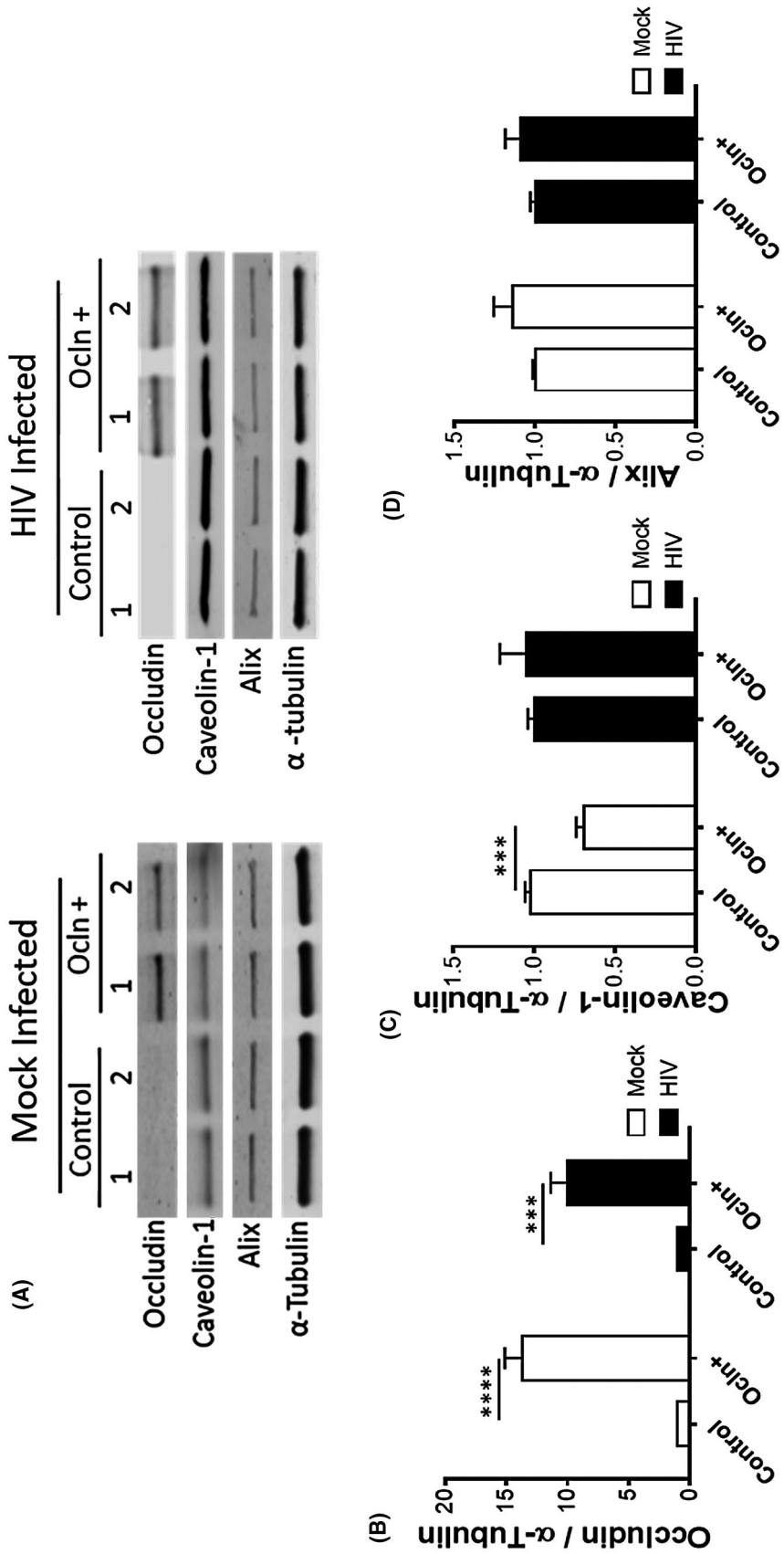
FIGURE 4 HIV-1 infection obliterates ocln-mediated regulation of cav-1 expression. Pericytes were transfected with 2 μg ocln expression vector per 10^6 cells and either mock-infected or HIV-1-infected with 60 ng/mL HIV-1 p24 for 48 h. The expression of ocln, cav-1, and Alix was evaluated by immunoblotting (A) and compared among groups. Tubulin was used as a loading control. Ocln overexpression (B) resulted in downregulation of cav-1 in mock-infected pericytes and this effect was obliterated in HIV-1-infected pericytes (C). Ocln overexpression did not affect Alix levels (D). Graphs indicate the mean ± SD from three independent experiments. ****$P < .0001$, ***$P = .0002$, n = 4-9 per group
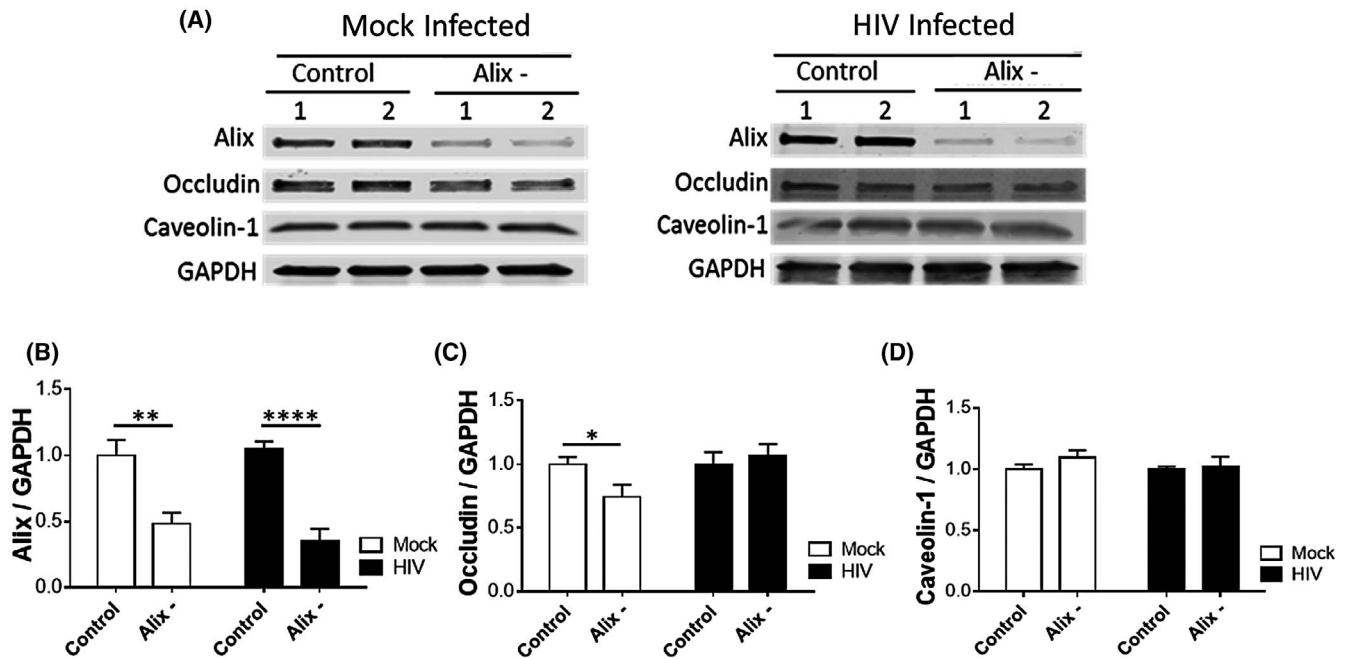
FIGURE 5 HIV-1 infection obliterates Alix-mediated regulation of ocln expression. Pericytes were transfected with 1 μg Alix siRNA per 10^6 cells and either mock-infected or HIV-1-infected with 60 ng/mL HIV-1 p24 for 48 h. The expression of Alix, ocln, and cav-1 was evaluated by immunoblotting (A) and compared among groups. GAPDH was used as a loading control. Alix silencing (B) resulted in downregulation of ocln in mock-infected pericytes and this effect was obliterated in HIV-1-infected pericytes (C). Alix silencing did not affect cav-1 levels (D). Graphs indicate the mean ± SD from three independent experiments. ****$P < .0001$, **$P = .003$, *$P < .0449$, n = 4-9 per group

non-detectable in the media. In addition, no significant differences were found in IL-12, IL-17A, IL-1ra, IL-5, IL-7, and VEGF among the employed experimental groups. The levels of anti-inflammatory INF-γ, IL-10, IL-15, and G-CSF were significantly decreased in cell culture media of HIV-1-infected pericytes (Figure 7A-D, respectively), while the levels of pro-inflammatory IL-6, MCP-1 (CCL2), and RANTES (CCL5) significantly increased after HIV-1 infection (Figure 7E-G, respectively). Overall, infection for 72 hours produced more advanced changes as compared to 48 hours post infection. In addition, media levels of INF-γ, G-CSF, RANTES, MIP1-β, and IP-10 significantly increased as the result of ocln overexpression (Figure 7A,D,G-I, respectively), while MCP-1 levels significantly decreased (Figure 7F).

4 | DISCUSSION

Prominent alterations of the BBB integrity that occur during HIV-1 infection[42,43] may contribute to the development of neurocognitive disorders in infected individuals. However, the direct interactions of HIV-1 with cells composing the BBB, and especially with BBB pericytes, are not well understood. Our group reported that brain pericytes express the main HIV-1 receptor, CD4, HIV-1 co-receptors CCR5 and CXCR4, and that these cells are prone to HIV-1 infection.[19] Several studies confirmed these results, identifying brain

pericytes as an important player in HIV-1 infection.[11,20,22,23,44] We recently proposed that pericytes might be HIV-1 reservoir cells in the CNS, as they can alternate from productive HIV-1 infection to latent steps of the viral cycle.[22] The importance of these findings stems from the fact that infection of pericytes may provide a gateway for HIV-1 to enter brain parenchyma. To support this notion, we demonstrated that HIV-1 is released from infected pericytes and can effectively infect new cell populations[20] (Figure 6).

Retroviruses such as HIV-1 evolve to modify the machinery of the host cell in order to promote all phases of viral life cycle, including egress from the cell. While HIV-1 entry and replication are relatively well understood, HIV-1 egress and the role of host cellular machinery in this process are understudied. In particular, no studies were performed on the mechanisms regulating HIV-1 egress from infected pericytes. The current study closes this gap and it is built on the premise that proteins involved in membrane plasticity, such as cav-1, ocln, and/or Alix can be subjected to HIV-1-mediated regulation, and in turn, influence HIV-1 life cycle and active infection. Indeed, a correlation between the time lapsed HIV-1 infection of pericytes and the expression levels of cav-1, ocln, and Alix was found in the present study. Specifically, ocln expression significantly decreased 48 hours after infection, followed by elevated levels at the later stages of infection, such as 72 hours. Cav-1 expression levels were found to be unaltered 48 hours following HIV-1 infection; however, they were significantly increased at 72 hours. Finally, Alix expression
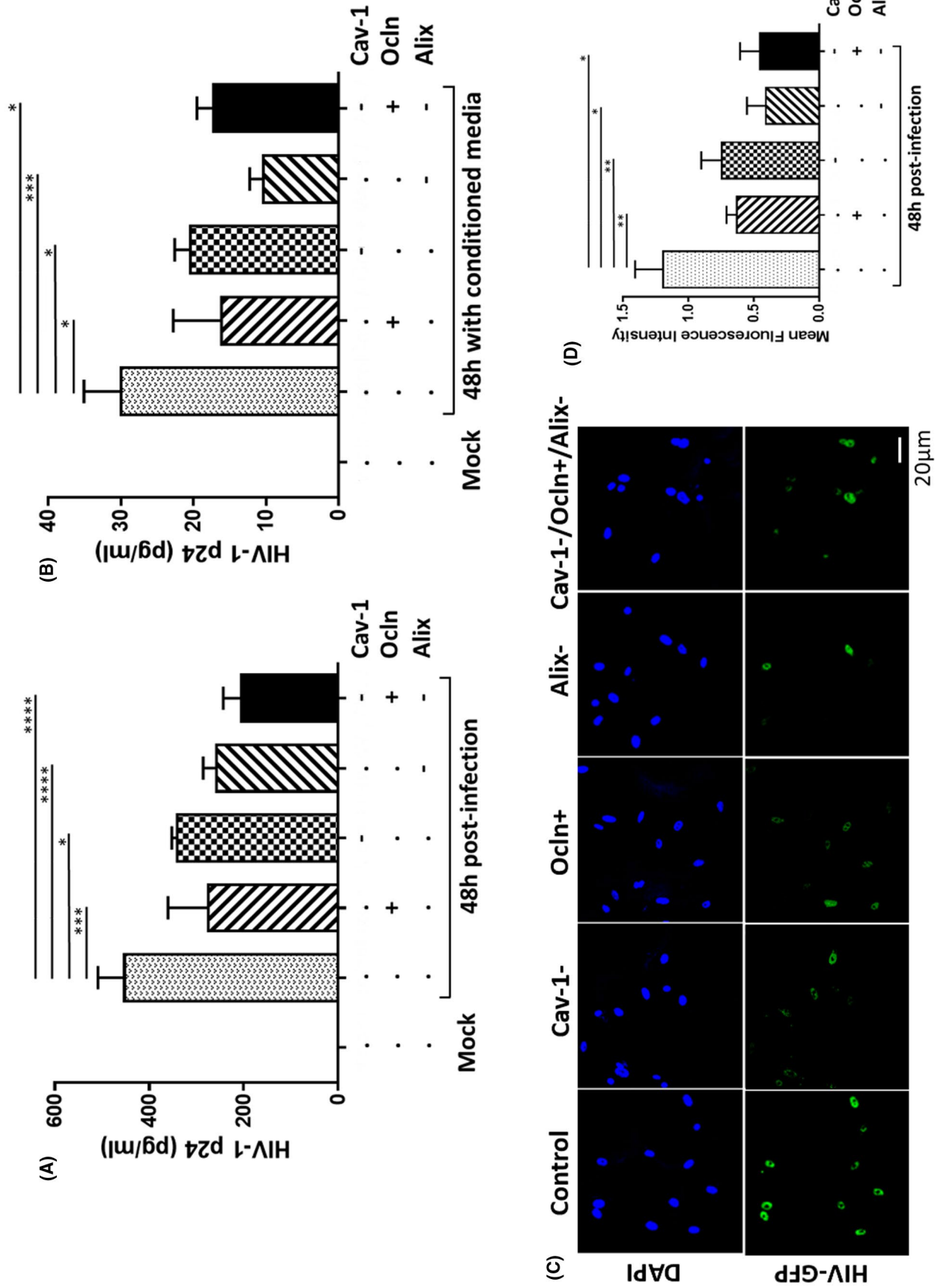
FIGURE 6 Modifications of the cav-1-ocln-Alix complex regulates HIV-1 infection. A, Pericytes were transfected with cav-1 siRNA (1 μg), ocln expression vector (2 μg), or/and Alix siRNA (1 μg) per 10[6] cells. When treatment with all three agents was combined, they were used at half the concentrations. Transfected cultures were then either mock-infected or HIV-1-infected as in Figure 1 and p24 levels in the media from pericyte cultures exposed to conditioned media from (A) for 48 h. C, Confocal microscopy images of HIV-1 pNL4-3-GFP-infected pericytes after ocln overexpression, cav-1 silencing, and Alix silencing. Nuclei were stained with DAPI (blue). GFP fluorescence (green) reflects HIV-1 transcription. D, Quantification of the mean fluorescence intensity (MFI) of GFP from (C). Data represents mean ± SEM from two independent experiments. $****P < .0001$, $***P = .0002$, $**P = .003$, $*P < .0449$, n = 4 per group. Scale bars, 20 μm
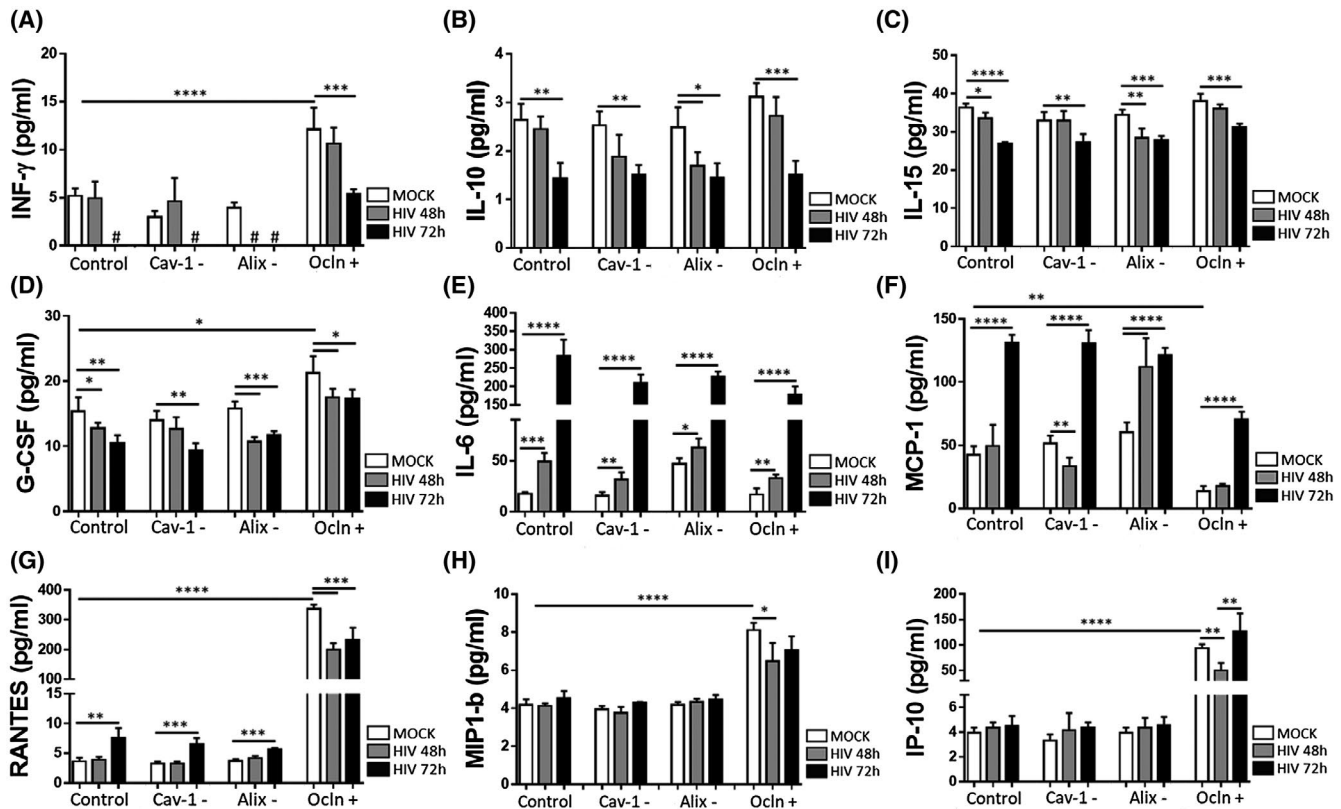
FIGURE 7 HIV-1 infection and/or modifications of the cav-1/ocln/Alix complex affect anti- and pro-inflammatory cytokine profile in pericytes. Pericytes were transfected with cav-1 siRNA (Cav-1-), ocln expression vector (Ocln+), or Alix siRNA (Alix-) as in Figure 5 and either mock-infected or HIV-1-infected for 48 or 72 h. Cytokine levels were analyzed in cell culture media by Bio-Plex Pro Human Cytokine assay kit. INF-γ levels decreased to non-detectable (#) concentrations after HIV-1 infection in control, cav-1-, and Alix- pericyte cultures. The data are mean ± SEM from two independent experiments. ****P < .0001, ***P = .0002, **P = .003, *P < .0449, n = 4 per group

levels demonstrated a direct correlation with the time lapsed following HIV-1 infection as they steadily increased both 48 and 72 hours after infection (Figure 1).

Taking into consideration the coordinated responses of cav-1, ocln, and Alix in response to HIV-1 infection, we next hypothesized that they may form a structural and/or functional complex that plays a role in HIV-1 life cycle. Our novel results indicate that cav-1, ocln, and Alix co-immunoprecipitate with each other and colocalize in human brain pericytes (Figure 2). These findings agree with the report that cav-1 can co-immunoprecipitate with ocln[45,46] in MDCK II cells and that these proteins also associate in T84 monolayers.[47] Studies have also indicated that cav-1-dependent endocytosis may play an important role in epithelial TJ dynamics, particularly in the regulation of ocln endocytosis. It was demonstrated that this process followed myosin light-chain kinase (MLCK) activation and appeared to be necessary for TNF-induced regulation of TJ composition and function.[36,48] In addition, cav-1 was shown to be involved in ocln recycling in brain endothelial cells.[49] However, the formation of the cav-1-ocln complex in non-barrier forming cells, such as pericytes, as well as the presence of Alix in this complex are novel observations.

Our novel results indicated that cav-1, ocln, and Alix not only form a multi-protein complex, but also cross-regulate each other's expression (Figures 3-5). Specifically, the levels of cav-1 influenced ocln expression but not Alix levels. Ocln levels had a strong regulatory impact on cav-1 expression but did not affect Alix. On the contrary, Alix expression influenced cellular ocln levels. HIV-1 infection diminished the regulatory abilities of the individual components of this complex to influence each other's expression. Nevertheless, the cav-1-ocln-Alix complex was preserved even in infected pericytes.

In order to further clarify the role of the cav-1, ocln, and/or Alix in HIV-1 infection, we investigated if modification of the expression of these proteins can impact viral replication and production of the HIV-1 capsid protein p24, the indicator of active HIV-1 infection. Our compelling and novel data indicates that silencing cav-1 can attenuate the transcriptional efficiency and the active production of p24 by HIV-1-infected pericytes (Figure 6). These results support the notion that the multifaceted functions of cav-1 may be involved in the pathogenesis of HIV-1 infection. For example, it has been reported that HIV-1 infection upregulates the expression of cav-1 in macrophages.[50] Cav-1 could serve as an early,

critical modulator responsible for signaling pathways that results in the disruption of TJs proteins. Contrasting our results, selected reports have demonstrated that cav-1 overexpression inhibits HIV-1 replication in macrophages.[28] Other studies, however, have suggested that cav-1 may serve as an effective target for protecting against HIV-1-related disruption of the BBB.[51] Silencing the cav-1 gene has also been described as having a key role in protecting against HIV-1 by defending against HIV-1 Tat-induced downregulation of ocln.[52]

Modification of the cav-1-ocln-Alix complex by overexpression of ocln also resulted in a prominent decrease in p24 levels in HIV-1-infected pericyte cultures (Figure 6). These findings are consistent with our reports[25] in which we characterized ocln as a novel NADH oxidase that inhibits HIV-1 transcription by controlling SIRT-1 expression and activation in human brain pericytes. The inverse relationship between ocln and HIV-1 transcription was further substantiated when it was shown that occludin silencing resulted in 75% and 250% increase in viral transcription in human primary macrophages and differentiated monocytic U937 cells, respectively.[25]

Like cav-1, silencing Alix also resulted in a decrease in p24 release and HIV-1 egress by infected pericytes (Figure 6). Alix is a part of ESCRT machinery, and its interaction with HIV-1 has been described.[53] However, the exact role and function of Alix in HIV-1 life cycle remain elusive. Some studies suggested that Alix has only a minor effect on HIV-1 budding.[54-56] However, other reports described an integral role of Alix in HIV-1 release and increased virus production.[57-59] The results of the current study are consistent with the latter observations. Indeed, among the components of the cav-1-ocln-Alix complex, the most prominent impact on decreasing p24 levels was observed upon Alix silencing.

Patients living with HIV-1 suffer from inflammatory conditions[41]; therefore, we evaluated the expression level of cytokines produced by pericytes upon modification of the cav-1-ocln-Alix complex in mock-infected and HIV-1-infected pericytes. Our results indicated that the levels IL-10, IL-15, INF-γ, and G-CSF were lower in HIV-1-infected pericytes in comparison to mock-infected pericytes. In contrast, IL-6, MCP-1/CCL-2, and RANTES exhibited elevated levels when pericytes were infected with HIV-1. These results concur with the well-established anti-inflammatory role of IL-10 and the pro-inflammatory impact of IL-6, MCP-1, and RANTES,[60,61] whose expression has been correlated with HIV-1 replication.[62] In the case of INF-γ, several studies suggested its anti-inflammatory role in the CNS,[63] and G-CSF has been described either as an anti- or pro-inflammatory cytokine, and/or immunomodulatory factor that suppresses the production of pro-inflammatory cytokines.[64-66]

In addition to changes in cytokine profiles due to HIV-1 infection, we also observed profound alterations of cytokine production upon modification of the cav-1-ocln-Alix complex. Specifically, ocln overexpression resulted in elevation of RANTES, INF-γ, G-CSF, MIP1-b, and IP-10, as well as a decrease in MCP-1/CCL-2. These patterns of change reflect both strong anti- and pro-inflammatory responses. The role of RANTES, INF-γ, MCP-1/CCL2, and G-CSF in HIV-1 infection was addressed above. MIP1 plays a role as an HIV-1-suppressive factor[67]; contrarily, IL-10 is pro-inflammatory and induces chemotaxis, apoptosis, cell growth, and angiostasis by binding to the CXCR3 receptor. These results confirm the impact of both HIV-1 infection and the cav-1-ocln-Alix complex on the cytokines profile, which includes stimulation of both anti- and pro-inflammatory cytokines, and, as such, is likely to modulate the overall neuroinflammatory responses in HIV-1-infected brains.

In conclusion, we have described for the first time that cav-1, ocln, and Alix form a multi-protein complex in human brain pericytes. These proteins can regulate each other, and their interactions are affected upon HIV-1 infection. Additionally, we presented evidence that modulation of the cav-1-ocln-Alix complex results in diminished HIV-1 replication. These findings provide novel cellular mechanisms involved in HIV-1 infection of brain pericytes that contribute to a better understanding of the pathology of brain infection by HIV-1 and the associated neuroinflammatory responses.

CONFLICT OF INTEREST

The authors declare no conflicts of interest.

AUTHOR CONTRIBUTIONS

ST, MP, and MT designed the research study. ST, MP, and SR performed and analyzed the immunoblotting, immunoprecipitation, and immunostaining experiments. ST produced HIV-1 virus, performed infections and all ELISA assays. AM designed the PyMol diagram. ST, SR, and MT wrote the manuscript and all authors revised it.

REFERENCES

1. Hill J, Rom S, Ramirez SH, Persidsky Y. Emerging roles of pericytes in the regulation of the neurovascular unit in health and disease. *J Neuroimmune Pharmacol*. 2014;9:591-605.
2. Armulik A, Mae M, Betsholtz C. Pericytes and the blood-brain barrier: recent advances and implications for the delivery of CNS therapy. *Ther Deliv*. 2011;2:419-422.

3. Mathiisen TM, Lehre KP, Danbolt NC, Ottersen OP. The perivascular astroglial sheath provides a complete covering of the brain microvessels: an electron microscopic 3D reconstruction. *Glia*. 2010;58:1094-1103.

4. Sa-Pereira I, Brites D, Brito MA. Neurovascular unit: a focus on pericytes. *Mol Neurobiol*. 2012;45:327-347.

5. Bell RD, Winkler EA, Sagare AP, et al. Pericytes control key neurovascular functions and neuronal phenotype in the adult brain and during brain aging. *Neuron*. 2010;68:409-427.

6. Kamouchi M, Ago T, Kitazono T. Brain pericytes: emerging concepts and functional roles in brain homeostasis. *Cell Mol Neurobiol*. 2011;31:175-193.

7. Guerra DAP, Paiva AE, Sena IFG, et al. Targeting glioblastoma-derived pericytes improves chemotherapeutic outcome. *Angiogenesis*. 2018;21:667-675.

8. Sena IFG, Paiva AE, Prazeres P, et al. Glioblastoma-activated pericytes support tumor growth via immunosuppression. *Cancer Med*. 2018;7:1232-1239.

9. Hamilton NB, Attwell D, Hall CN. Pericyte-mediated regulation of capillary diameter: a component of neurovascular coupling in health and disease. *Front Neuroenergetics*. 2010;2:5.

10. Winkler EA, Bell RD, Zlokovic BV. Central nervous system pericytes in health and disease. *Nat Neurosci*. 2011;14:1398-1405.

11. Cho HJ, Kuo AM, Bertrand L, Toborek M. HIV alters gap junction-mediated intercellular communication in human brain pericytes. *Front Mol Neurosci*. 2017;10:410.

12. Bhowmick S, D'Mello V, Caruso D, Wallerstein A, Abdul-Muneer PM. Impairment of pericyte-endothelium crosstalk leads to blood-brain barrier dysfunction following traumatic brain injury. *Exp Neurol*. 2019;317:260-270.

13. Heldin CH. Targeting the PDGF signaling pathway in tumor treatment. *Cell Commun Signal*. 2013;11:97.

14. Sagare AP, Bell RD, Zhao Z, et al. Pericyte loss influences Alzheimer-like neurodegeneration in mice. *Nat Commun*. 2013;4:2932.

15. Winkler EA, Sengillo JD, Sullivan JS, Henkel JS, Appel SH, Zlokovic BV. Blood-spinal cord barrier breakdown and pericyte reductions in amyotrophic lateral sclerosis. *Acta Neuropathol*. 2013;125:111-120.

16. Toborek M, Lee YW, Flora G, et al. Mechanisms of the blood-brain barrier disruption in HIV-1 infection. *Cell Mol Neurobiol*. 2005;25:181-199.

17. Gonzalez-Mariscal L, Betanzos A, Avila-Flores A. MAGUK proteins: structure and role in the tight junction. *Semin Cell Dev Biol*. 2000;11:315-324.

18. Tsukita S, Furuse M, Itoh M. Multifunctional strands in tight junctions. *Nat Rev Mol Cell Biol*. 2001;2:285-293.

19. Nakagawa S, Castro V, Toborek M. Infection of human pericytes by HIV-1 disrupts the integrity of the blood-brain barrier. *J Cell Mol Med*. 2012;16:2950-2957.

20. Castro V, Bertrand L, Luethen M, et al. Occludin controls HIV transcription in brain pericytes via regulation of SIRT-1 activation. *FASEB J*. 2016;30:1234-1246.

21. Persidsky Y, Hill J, Zhang M, et al. Dysfunction of brain pericytes in chronic neuroinflammation. *J Cereb Blood Flow Metab*. 2016;36:794-807.

22. Bertrand L, Cho HJ, Toborek M. Blood-brain barrier pericytes as a target for HIV-1 infection. *Brain*. 2019;142:502-511.

23. Bohannon DG, Ko A, Filipowicz AR, Kuroda MJ, Kim WK. Dysregulation of sonic hedgehog pathway and pericytes in the brain after lentiviral infection. *J Neuroinflammation*. 2019;16:86.

24. Blasig IE, Bellmann C, Cording J, et al. Occludin protein family: oxidative stress and reducing conditions. *Antioxid Redox Signal*. 2011;15:1195-1219.

25. Castro V, Skowronska M, Lombardi J, et al. Occludin regulates glucose uptake and ATP production in pericytes by influencing AMP-activated protein kinase activity. *J Cereb Blood Flow Metab*. 2018;38:317-332.

26. Huang Q, Zhong W, Hu Z, Tang X. A review of the role of cav-1 in neuropathology and neural recovery after ischemic stroke. *J Neuroinflammation*. 2018;15:348.

27. Llano M, Kelly T, Vanegas M, et al. Blockade of human immunodeficiency virus type 1 expression by caveolin-1. *J Virol*. 2002;76:9152-9164.

28. Wang XM, Nadeau PE, Lin S, Abbott JR, Mergia A. Caveolin 1 inhibits HIV replication by transcriptional repression mediated through NF-kappaB. *J Virol*. 2011;85:5483-5493.

29. Mergia A. The role of caveolin 1 in HIV infection and pathogenesis. *Viruses*. 2017;9:129.

30. Gargalovic P, Dory L. Cellular apoptosis is associated with increased caveolin-1 expression in macrophages. *J Lipid Res*. 2003;44:1622-1632.

31. Galbiati F, Volonte D, Liu J, et al. Caveolin-1 expression negatively regulates cell cycle progression by inducing G(0)/G(1) arrest via a p53/p21(WAF1/Cip1)-dependent mechanism. *Mol Biol Cell*. 2001;12:2229-2244.

32. Harris J, Werling D, Hope JC, Taylor G, Howard CJ. Caveolae and caveolin in immune cells: distribution and functions. *Trends Immunol*. 2002;23:158-164.

33. Uittenbogaard A, Everson WV, Matveev SV, Smart EJ. Cholesteryl ester is transported from caveolae to internal membranes as part of a caveolin-annexin II lipid-protein complex. *J Biol Chem*. 2002;277:4925-4931.

34. Zou H, Stoppani E, Volonte D, Galbiati F. Caveolin-1, cellular senescence and age-related diseases. *Mech Ageing Dev*. 2011;132:533-542.

35. Lamaze C, Torrino S. Caveolae and cancer: a new mechanical perspective. *Biomed J*. 2015;38:367-379.

36. Marchiando AM, Shen L, Graham WV, et al. Caveolin-1-dependent occludin endocytosis is required for TNF-induced tight junction regulation in vivo. *J Cell Biol*. 2010;189:111-126.

37. Dowlatshahi DP, Sandrin V, Vivona S, et al. ALIX is a Lys63-specific polyubiquitin binding protein that functions in retrovirus budding. *Dev Cell*. 2012;23:1247-1254.

38. Fujii K, Hurley JH, Freed EO. Beyond Tsg101: the role of Alix in 'ESCRTing' HIV-1. *Nat Rev Microbiol*. 2007;5:912-916.

39. Van Duyne R, Kuo LS, Pham P, Fujii K, Freed EO. Mutations in the HIV-1 envelope glycoprotein can broadly rescue blocks at multiple steps in the virus replication cycle. *Proc Natl Acad Sci U S A*. 2019;116:9040-9049.

40. Ku PI, Bendjennat M, Ballew J, Landesman MB, Saffarian S. ALIX is recruited temporarily into HIV-1 budding sites at the end of gag assembly. *PLoS One*. 2014;9:e96950.

41. Nemeth CL, Bekhbat M, Neigh GN. Neural effects of inflammation, cardiovascular disease, and HIV: parallel, perpendicular, or progressive? *Neuroscience*. 2015;302:165-173.

42. Giovannoni G, Miller RF, Heales SJ, Land JM, Harrison MJ, Thompson EJ. Elevated cerebrospinal fluid and serum nitrate and nitrite levels in patients with central nervous system complications of HIV-1 infection: a correlation with blood-brain-barrier dysfunction. *J Neurol Sci*. 1998;156:53-58.

43. McArthur JC, Nance-Sproson TE, Griffin DE, et al. The diagnostic utility of elevation in cerebrospinal fluid beta 2-microglobulin in HIV-1 dementia. Multicenter AIDS Cohort Study. *Neurology*. 1992;42:1707-1712.

44. Piekna-Przybylska D, Nagumotu K, Reid DM, Maggirwar SB. HIV-1 infection renders brain vascular pericytes susceptible to the extracellular glutamate. *J Neurovirol*. 2019;25:114-126.

45. Lynch RD, Francis SA, McCarthy KM, Casas E, Thiele C, Schneeberger EE. Cholesterol depletion alters detergent-specific solubility profiles of selected tight junction proteins and the phosphorylation of occludin. *Exp Cell Res*. 2007;313:2597-2610.

46. Itallie CM, Anderson JM. Caveolin binds independently to claudin-2 and occludin. *Ann N Y Acad Sci*. 2012;1257:103-107.

47. Nusrat A, Parkos CA, Verkade P, et al. Tight junctions are membrane microdomains. *J Cell Sci*. 2000;113(Pt 10):1771-1781.

48. Shen L, Turner JR. Actin depolymerization disrupts tight junctions via caveolae-mediated endocytosis. *Mol Biol Cell*. 2005;16:3919-3936.

49. Park M, Hennig B, Toborek M. Methamphetamine alters occludin expression via NADPH oxidase-induced oxidative insult and intact caveolae. *J Cell Mol Med*. 2012;16:362-375.

50. Lin S, Wang XM, Nadeau PE, Mergia A. HIV infection upregulates caveolin 1 expression to restrict virus production. *J Virol*. 2010;84:9487-9496.

51. Zhong Y, Smart EJ, Weksler B, Couraud PO, Hennig B, Toborek M. Caveolin-1 regulates human immunodeficiency virus-1 Tat-induced alterations of tight junction protein expression via modulation of the Ras signaling. *J Neurosci*. 2008;28:7788-7796.

52. Zou M, Huang W, Jiang W, Wu Y, Chen Q. Role of Cav-1 in HIV-1 tat-induced dysfunction of tight junctions and Abeta-transferring proteins. *Oxid Med Cell Longev*. 2019;2019:3403206.

53. Usami Y, Popov S, Gottlinger HG. Potent rescue of human immunodeficiency virus type 1 late domain mutants by ALIX/AIP1 depends on its CHMP4 binding site. *J Virol*. 2007;81:6614-6622.

54. Gottlinger HG, Dorfman T, Sodroski JG, Haseltine WA. Effect of mutations affecting the p6 gag protein on human immunodeficiency virus particle release. *Proc Natl Acad Sci U S A*. 1991;88:3195-3199.

55. Martin-Serrano J, Yarovoy A, Perez-Caballero D, Bieniasz PD. Divergent retroviral late-budding domains recruit vacuolar protein sorting factors by using alternative adaptor proteins. *Proc Natl Acad Sci U S A*. 2003;100:12414-12419.

56. Demirov DG, Ono A, Orenstein JM, Freed EO. Overexpression of the N-terminal domain of TSG101 inhibits HIV-1 budding by blocking late domain function. *Proc Natl Acad Sci U S A*. 2002;99:955-960.

57. Strack B, Calistri A, Craig S, Popova E, Gottlinger HG. AIP1/ALIX is a binding partner for HIV-1 p6 and EIAV p9 functioning in virus budding. *Cell*. 2003;114:689-699.

58. Munshi UM, Kim J, Nagashima K, Hurley JH, Freed EO. An Alix fragment potently inhibits HIV-1 budding: characterization of binding to retroviral YPXL late domains. *J Biol Chem*. 2007;282:3847-3855.

59. Fisher RD, Chung HY, Zhai Q, Robinson H, Sundquist WI, Hill CP. Structural and biochemical studies of ALIX/AIP1 and its role in retrovirus budding. *Cell*. 2007;128:841-852.

60. Wojdasiewicz P, Poniatowski LA, Szukiewicz D. The role of inflammatory and anti-inflammatory cytokines in the pathogenesis of osteoarthritis. *Mediators Inflamm*. 2014;2014:561459.

61. Wood S, Jayaraman V, Huelsmann EJ, et al. Pro-inflammatory chemokine CCL2 (MCP-1) promotes healing in diabetic wounds by restoring the macrophage response. *PLoS One*. 2014;9:e91574.

62. Gonzalez E, Rovin BH, Sen L, et al. HIV-1 infection and AIDS dementia are influenced by a mutant MCP-1 allele linked to increased monocyte infiltration of tissues and MCP-1 levels. *Proc Natl Acad Sci U S A*. 2002;99:13795-13800.

63. Miller NM, Wang J, Tan Y, Dittel BN. Anti-inflammatory mechanisms of IFN-gamma studied in experimental autoimmune encephalomyelitis reveal neutrophils as a potential target in multiple sclerosis. *Front Neurosci*. 2015;9:287.

64. Bordoni V, Sacchi A, Casetti R, et al. Impact of ART on dynamics of growth factors and cytokines in primary HIV infection. *Cytokine*. 2019;125:154839.

65. Boneberg EM, Hartung T. Molecular aspects of anti-inflammatory action of G-CSF. *Inflamm Res*. 2002;51:119-128.

66. Bhattacharya P, Budnick I, Singh M, et al. Dual role of GM-CSF as a pro-inflammatory and a regulatory cytokine: implications for immune therapy. *J Interferon Cytokine Res*. 2015;35:585-599.

67. Cocchi F, DeVico AL, Garzino-Demo A, Arya SK, Gallo RC, Lusso P. Identification of RANTES, MIP-1 alpha, and MIP-1 beta as the major HIV-suppressive factors produced by CD8+ T cells. *Science*. 1995;270:1811-1815.